

ACCEPTED MANUSCRIPT • OPEN ACCESS

## Linestrength ratio spectroscopy as a new primary thermometer for redefined Kelvin dissemination

To cite this article before publication: Luigi Santamaria Amato *et al* 2019 *New J. Phys.* in press <https://doi.org/10.1088/1367-2630/ab4d07>

### Manuscript version: Accepted Manuscript

Accepted Manuscript is “the version of the article accepted for publication including all changes made as a result of the peer review process, and which may also include the addition to the article by IOP Publishing of a header, an article ID, a cover sheet and/or an ‘Accepted Manuscript’ watermark, but excluding any other editing, typesetting or other changes made by IOP Publishing and/or its licensors”

This Accepted Manuscript is © 2019 The Author(s). Published by IOP Publishing Ltd on behalf of Deutsche Physikalische Gesellschaft and the Institute of Physics.

As the Version of Record of this article is going to be / has been published on a gold open access basis under a CC BY 3.0 licence, this Accepted Manuscript is available for reuse under a CC BY 3.0 licence immediately.

Everyone is permitted to use all or part of the original content in this article, provided that they adhere to all the terms of the licence <https://creativecommons.org/licenses/by/3.0>

Although reasonable endeavours have been taken to obtain all necessary permissions from third parties to include their copyrighted content within this article, their full citation and copyright line may not be present in this Accepted Manuscript version. Before using any content from this article, please refer to the Version of Record on IOPscience once published for full citation and copyright details, as permissions may be required. All third party content is fully copyright protected and is not published on a gold open access basis under a CC BY licence, unless that is specifically stated in the figure caption in the Version of Record.

View the [article online](#) for updates and enhancements.

# Linestrength ratio spectroscopy as a new primary thermometer for redefined Kelvin dissemination

Luigi Santamaria Amato<sup>1</sup>, Mario Siciliani de Cumis<sup>†1</sup>,  
Giuseppe Bianco<sup>1</sup>, Raffaele Pastore<sup>2</sup>, Pablo Cancio Pastor<sup>3§</sup>

<sup>1</sup>ASI, Agenzia Spaziale Italiana, Centro di Geodesia Spaziale, Matera 75100, Italy

<sup>2</sup>Department of Chemical, Materials and Production Engineering, University of Naples Federico II, P. le Tecchio 80 -80125- Napoli, Italy

<sup>3</sup>CNR-INO, Istituto Nazionale di Ottica, Via N. Carrara 1, 50019 Sesto Fiorentino, Italy

**Abstract.** Experimental methods for primary thermometry, after Kelvin unit redefinition on May 2019, become based on a known value of the Boltzmann constant rather than by measuring temperature with respect to a reference point. In this frame, we propose Linestrength Ratio Thermometry (LRT) as a candidate method for primary thermometry in the 9-700 K temperature range. Temperature accuracies at the ppm level are prospected for LRT applied to optical transitions of the CO molecule in the range 80-700 K and of a rare-earth-doped crystal in the 9-100 K one. Future implementations of this technique can contribute to measure the calibration-discrepancies in the ITS-90 metrological scale of thermodynamic temperature which can have a measurable impact in applications ranging from fundamental-physics to meteorology and climatology.

*Keywords:* Molecular spectroscopy, primary thermometry, laser spectroscopy, carbon monoxide, rare earth doped crystal, Kelvin dissemination

<sup>†</sup> Corresponding author: mario.sicilianidecumis@asi.it

<sup>§</sup> Corresponding author: pablo.canciopastor@ino.it

## 1. Introduction

Nowadays, the measurement of thermodynamic temperature  $T$  of physical systems plays a fundamental role in experimental science ranging from fundamental physics [1, 2, 3, 4] to chemical physics [5, 6, 7, 8, 9], cold atoms physics [10, 11, 12], meteorology and climatology [13, 14] and control of industrial processes. Accuracy and reproducibility of such measurements depends on the international standard of temperature; the Kelvin unit and its precise traceability.

Up to now, the International System (SI) of units has defined the Kelvin in terms of the temperature of the triplet point of "pure" water, which was assigned the exact value of  $T_{TPW} = 273.16$  K. It was the absolute reference value for each accurate thermodynamic temperature measurement, traceable through the primary thermometers (PT's). In these thermometers, there is a basic relation between the observable and  $T$  that can be written down explicitly without having to introduce unknown, temperature-dependent quantities. The PT's are impractical for most part of the applications that need accurate  $T$  measurements due to their size, measurement speed and cost. Instead, secondary thermometers (ST's), as the platinum resistance temperature detector (RTD), are the practical-instrumentation used to measure precisely thermodynamic temperature. But such a thermometers must be calibrated against a defined fixed temperature points to ensure worldwide accuracy and primary traceability. Indeed, the International Temperature Scale of 1990 (ITS-90 [15]) and the Provisional Low Temperature Scale of 2000 (PLTS-2000 [16]) were established by the Consultative Committee for Thermometry (CCT) of the International Committee for Weights and Measures (CIPM) as a practical reference scales for dissemination of the Kelvin unit. These scales have a number of fixed temperature values defined by the reproducible freezing or melting temperature of pure substances measured against  $T_{TPW}$  by means of accepted primary thermometers.

On May 2019, the CIPM has anticipated the most radical revision of the definition of the SI base units in terms of exact fundamental constants, and in particular the Kelvin unit in terms of the assigned exact value of the Boltzmann constant,  $k$  [17, 18]. The *mise en pratique* for the Kelvin redefinition (*MeP-K-19*) establishes, as first, that the accurate methods used to determine  $k$  [19, 20, 21, 22, 23], become PT's [24] because in their basic equations  $T$  always appears as thermal energy  $kT$ . Recently, we proposed Linestrength Ratio Thermometry (LRT) [25] to determine Boltzmann constant with accuracy comparable or even better than other primary techniques. Consequently, we propose the LRT method as a potential candidate as a primary thermometer, prospecting its accuracy and precision performances to measure some reference temperatures of the ITS-90, and by extending the application towards the low  $T$  range where other optical techniques are not available. Secondly, by *MeP-K-19*, the worldwide dissemination of Kelvin will be provided equally by those PT's and through the defined scales ITS-90 and PLTS-2000. In this way the practice of thermometry will remain largely unchanged with a smoothed impact in the calibration

of secondary thermometers and the T-measurement-based applications. The first immediate implication on the scales of the new definition is that the  $T_{TPW}$  would lose its status of reference temperature of the primary thermometry, becoming just another fixed T point. The uncertainty of such point would be the order of  $10^{-4}$  K transferred by the  $k$  uncertainty at the moment of the redefinition. Because  $T_{TPW}$  still remains the reference point for the ITS-90, this uncertainty will be propagated to the other fixed points of the scale with a larger impact in the extreme T's. The new PT's are called to calibrate these uncertainties as first issue.

Equally important for a proper Kelvin dissemination is to calibrate systematic discrepancies,  $T-T_{90}$  between temperature points of the ITS-90 ( $T_{90}$ ) and the measured T by using the new defined PT's [26, 27]. Although such systematic errors seem to be small if compared with precision of secondary thermometers, they can produce measurable effects in applications that need precise temperature determinations. For example measured shift of  $1.5 \times 10^{-4}$  of  $T-T_{90}$  for temperatures in the range of meteorological relevance (-50 to 90 °C), even if smaller than the T-variations of the ST's in the short time due to other environment factors, might be just detectable in homogenisation procedures using annual or decadal means [27]. More important, the metrological relevance of these discrepancies prospects a possible future revision of the ITS-90, where current scale errors will certainly be removed if they takes place, and the temperatures estimated according the new ITS will be likely to be much closer to true (i.e. thermodynamic) temperature T than at the present.

In this framework, new accurate thermometry methods as LRT are welcome. To this aim, we report the prospected accuracy performances of LRT to measure absolute T's in the range between 9 and 700 K. The temperature uncertainties of some fixed points of the ITS-90 between triple point of argon (83.8058 K) and freezing point of zinc (692.677 K) were systematically evaluated by applying LRT to ro-vibrational transitions of the CO molecule. In addition, the applicability of LRT to measure T's in the low range of ITS-90 (9-100K) by laser spectroscopy in a rare-earth-doped crystal is proposed. Similar accuracy performances are also prospected in this temperature range

### LRT method for primary thermometry

LRT method is based on the precise measurement of the linestrength ratio,  $R$  of two transitions  $a$  and  $b$  of the targeted specie at two different temperatures,  $T$  and  $T_r$ :  $R(T) = \frac{S_b(T)}{S_a(T)}$ ,  $R(T_r) = \frac{S_b(T_r)}{S_a(T_r)}$ , with  $S_{a,b}$  linestrengths of the  $a$ ,  $b$  transitions, respectively [25]. Laser absorption spectroscopy experiments in highly controlled temperature environment can be used to measure these ratios with high precision (few ppm). Other techniques [28, 29] based on the same principle but with different experimental implementation have been used to measure high temperatures with lower accuracy.

In LRT, a determination of the temperature  $T$  with respect to the other  $T_r$  is

obtained by:

$$T(\ln(F), T_r, \nu_a) = \frac{T_r h \nu_a}{T_r k \ln(F) + h \nu_a} \quad (1)$$

with  $F(T, T_r) \equiv \frac{R(T)}{R(T_r)}$ ,  $k$  Boltzmann constant and  $\nu_a$  the frequency corresponding to the energy of the lower level of the  $a$  transition, and by considering  $b$  as a ground state transition ( $\nu_b=0$ ) for simplicity. This equation was deduced by considering the relationship between the linestrengths of a transition at two different temperatures [30]. Hence, LRT can be considered to fulfill the *MeP-K-19* criteria of relative primary thermometry: Eq.1 is the simple equation to measure thermodynamic temperatures with respect to a reference one, in a wide temperature range with a low uncertainty  $\delta T$ :

$$\delta T = \sqrt{\delta T_r^2 + \delta F^2 + \delta \nu_a^2} \quad (2)$$

where  $\delta T_r = \frac{\partial T}{\partial T_r} dT_r$ ,  $\delta F = \frac{\partial T}{\partial F} dF$  and  $\delta \nu_a = \frac{\partial T}{\partial \nu_a} d\nu_a$ .

The experimental implementation of LRT uses two cells, highly stabilized at the  $T$ ,  $T_r$  temperatures to perform simultaneous absorption spectroscopic detection of the  $a$ ,  $b$  transitions with high resolution and signal-to-noise ratio (S/N). In this way, a precise measurement of  $F$  is achieved by numerical integration of the detected signals. Moreover, common systematic experimental effects present in individual spectroscopic measurements of linestrengths are removed by using the ratio approach, and hence improving the final uncertainty,  $dF$ . Nevertheless, it actually turns to be the limiting factor of the final error of  $T$  in LRT even if the functional dependence of  $T$  on  $F$ , according with Eq.1, shows a large slope and mitigates the  $F$ -error propagation: an uncertainty  $\delta F$  on  $F$  measurement corresponds to a small uncertainty  $\delta T$  on  $T$ . This is the strength of LRT as thermometric method which can be able to provide precise  $T$  measurements even if measuring a challenge parameter as the linestrength ratios of optical transitions.

The key criteria for LRT applicability as PT is to individuate the best combination of the transitions which minimize the total error given by eq. 2. In our previous paper [25], we did this evaluation with the aim of an accurate determination of  $k$  by LRT of the CO molecule at two known temperatures: the  $T_r=T_{TPW}$  and the triplet point temperature of Argon,  $T=T_{TPAr}$ . If LRT is used as PT, the individuated CO transitions in that case could be appropriated to measure  $T_{TPA}$  against  $T_{TPW}$  (or the contrary), but not for other temperature points of the ITS-90 scale. In view of a real PT applicability of LRT, now, we do a more exhaustive analysis both in terms possible transitions and targeted species to cover all  $T_{90}$  points in the range 9-700 K.

### LRT on CO molecule: primary thermometry in the 80-700 K range

To illustrate the performances of LRT as PT in this range, we have selected which is probably the most promising molecule: carbon monoxide. The reasons of that are the following:

140 - low freezing point (68.13 K) enabling wide range of applicability for LRT  
141 thermometry.

142 - As biatomic molecule, it shows a simple ro-vibrational spectrum in the mid-  
143 infrared (MIR) spectral region. As a consequence it is feasible to find target transitions  
144 with negligible interference effects by off-resonance absorptions of CO.

145 - ro-vibrational transitions in the MIR with large dipole moment, allowing strong  
146 absorption at low pressure.

147 In addition, the current availability of narrow linewidth laser sources [31, 32, 33] and  
148 high performance detection technology [34] in the MIR allow to perform high-resolution  
149 spectroscopy of CO transitions with very high S/N, as required to get low uncertainty  
150 on  $F$ .

### 151 *Selection of the LRT transitions*

152 In the following we describe the procedure to individuate the best transition of CO  
153 ( $a$  transition) to perform LRT primary thermometry in *defined points* of ITS-90 scale  
154 between 83.8058 and 692.677 K by considering  $T_r = T_{TPW}$  as reference temperature. The  
155 analysis is made in terms of minimum error  $\delta T$  evaluated by propagating the prospected  
156 errors in  $dT_r$ ,  $dF$  and  $d\nu_a$  for each considered CO transition. The R(0) of the (2-0)  
157 band of CO at 4263.837197  $\text{cm}^{-1}$  (having  $\nu_b=0$ ) is the  $b$  transition, common to all  
158 temperatures. Our algorithm downloads a list of linestrengths for the CO molecule in  
159 1000-10000  $\text{cm}^{-1}$  wavenumber range [35] and the corresponding energy (divided by  $h$ ) of  
160 lower state,  $\nu_a$  [36, 37] for each analyzed temperature, and calculates  $\delta T$  by using eq.2.  
161 In this calculation, we consider an experimental uncertainty on  $T_r$  of  $dT_r = 0.3$  mK, easily  
162 achievable by using temperature-controlled commercial cells. We assume to achieve a  
163 S/N of the CO spectra to allow a  $R$  measurement uncertainty at the best reported for  
164 absorption spectroscopy [23], i.e.  $dR/R = dR_r/R_r = 2.8$  ppm or  $dF/F = 4$  ppm.

165 For  $\nu_a$ ,  $d\nu_a$  is evaluated taken into account the error due to pressure shift for each  
166 transition in the pressure range of a practicable LRT experiment (around 10 Pascal)  
167 [37]. As shown in the following, this contribution should be considered negligible to the  
168 total T-error.

169 Let first analyzed the behaviour of T error with the spectral region by considering  
170 CO transitions from different vibrational bands. In Fig.1, the relative error  $\delta T/T$  for  
171  $T_{TPAr} = 83.8058$  K calculated for the CO ro-vibrational transitions of the fundamental,  
172 first and second overtone bands is shown, as well as the partial contributions  $\delta T_r/T$ ,  
173  $\delta F/T$  and  $\delta \nu_a/T$ . In all cases, the final error is dominated by the linestrength ratio  
174 uncertainty as expected. We note that similar relative temperature errors were found  
175 for transitions in the fundamental and overtone bands. This is fundamental in view of a  
176 practical implementation of LRT, because of the major availability of the laser, optics  
177 and optics and electro-optics technology at the wavelengths of overtone bands. Between  
178 them, the (2-0) band transitions are preferred to those of the (3-0) band due to the  
179 strong intensity of the former by considering the same final T-error level. For that, the

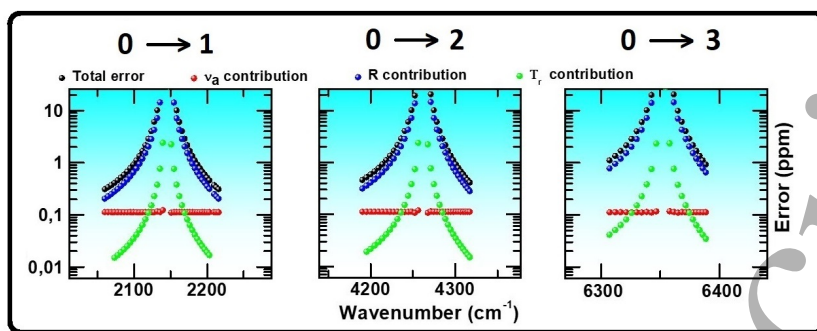


**Figure 1.** Relative error  $\delta T/T$  (black points) in ppm on temperature measurement of  $T_{TPAr}$  by LRT with  $T_{TPW}$  as reference temperature and by using different rotational transitions of the fundamental ( $0 < J < 16$ ) (left graph), first overtone ( $0 < J < 15$ ) (center graph) and second overtone ( $0 < J < 10$ ) (right graph) vibrational bands. Green, red and blue points for each graph are the partial contribution to this error due to the uncertainties of the reference temperature, frequency of the lower level of the transition and  $F$  ratio measurement, respectively ( $\delta T_r$ ,  $\delta \nu_a$  and  $\delta F$  contribution in eq.2).

180 final best  $a$  transition candidates were chosen from the first overtone (2-0).

181 The same procedure was applied to calculate  $\delta T$  for all the other analysed  
 182  $T_{90}$ 's: triple point of mercury,  $T_{TPHg} = 234,3156$  K; melting point of gallium,  
 183  $T_{MPGa} = 302.9146$  K; freezing point of indium,  $T_{FPIIn} = 429.7485$  K; freezing point of  
 184 tin,  $T_{FPSn} = 505.078$  K; freezing point of zinc,  $T_{FPZn} = 692.677$  K.

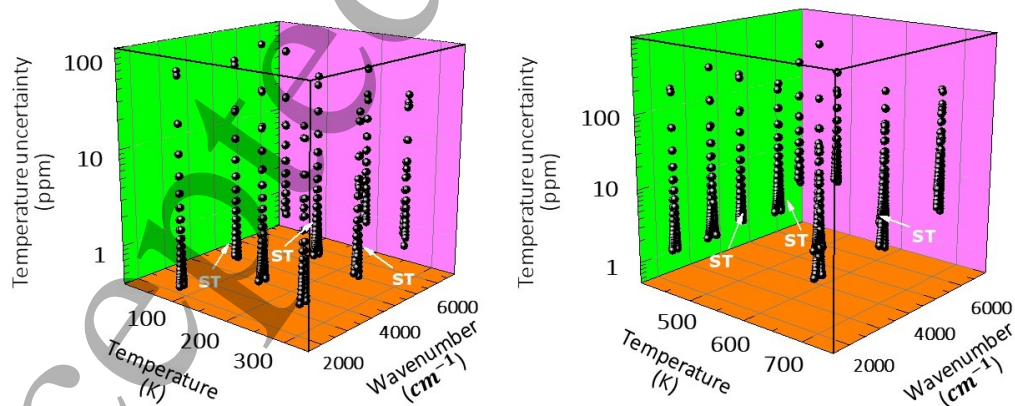


**Figure 2.** Total relative errors  $\delta T/T$  (z axis) for the entire temperature range (x axis: 80-350 K left graph, 350-700 K right graph) as function of transition wavenumber (y axis). The best transition for each ITS-90 in the 80-700 K range fixed point is indicated by ST and is proposed for LRT-temperature measurement with ppm accuracy.

**Table 1.** Prospected total relative temperature error of a LRT-measurement of ITS-90 fixed points in the range 83.8058-692.677 K with respect to the reference temperature  $T_{TPW}=273.1600$  (3) K.  $dF/F=4$  ppm was considered in this calculation

T (K)	a wavenumber (cm <sup>-1</sup> )	10 <sup>-22</sup> S <sub>a</sub> (T) (cm/mol)	b wavenumber (cm <sup>-1</sup> )	10 <sup>-22</sup> S <sub>b</sub> (T) (cm/mol)	$\delta T/T$ (ppm)
83.8058	4303.623335	2,004	4263.837197	2.459	0.79
234.3156	4324.409820	1.491	4263.837197	8.855	0.87
302,915	4328.878516	1.797	4263.837197	6.854	0.96
429,7485	4328.878516	4.942	4263.837197	4.831	1.3
505,078	4328.878516	6.827	4263.837197	4.105	1.6
692,677	4328.878516	10.42	4263.837197	2.964	2.2

$\delta T/T$  in the z-axis as function of the measured thermodynamic temperature T (x-axis) and the wavenumber of the transition (y-axis). All the three CO vibrational bands (fundamental and 1st and 2nd overtones) have been considered. The best transition for LRT determination of the T<sub>90</sub>'s at the ppm level (signed as ST in the Fig.2) was selected taking into account the criteria of minimum  $\delta T$  for transitions of the first overtone band, excluding those with linestrength lower than 10<sup>-22</sup> cm/mol. For the ST transitions, high S/N spectra can be allowed at low CO gas pressure in a technically better spectral region.

Considering these ST as the *a* transition candidates for LRT primary thermometry at the ITS-90 fixed temperatures between 80-700 K, we report in detail in Fig. 3 and Table 1, the prospected relative uncertainty  $\delta T/T$  by considering the T<sub>TPW</sub> as reference temperature. Data about linestrengths and wavenumbers of the *a* and *b* transitions for each temperature are included in Table 1. In Fig. 3, in addition, the main temperature error contributions due to  $dT_r$  and  $dF$  are shown. The F-contribution is the dominant source of error and it is almost constant in all considered temperature range. Instead, the T<sub>r</sub>-contribution begin to be consistent for T above 300 K, and it is almost negligible at low temperatures. Nevertheless, the total error is always lower than 2.5 ppm and becomes lower than 1 ppm for T under 300 K.

#### 204 *Uncertainty analysis on spectroscopic measurement of F ratios*

205 All the above analysis about uncertainties at ppm level on LRT primary thermometry  
 206 are supported if the considered experimental errors on  $\nu_a$ , T<sub>r</sub> and F are achieved. The  
 207  $\nu_a$  frequencies of the ST transitions are known with a relative accuracy of about 0.1 ppm  
 208 (see Fig.1) for the experimental conditions of the CO samples in LRT, and hence we  
 209 consider a negligible contribution of  $d\nu_a/\nu_a$  on T's at the ppm level. For T<sub>r</sub>, temperature  
 210 stability at the 0.3 mK level can be achieved with commercial control systems. Only  
 211 for above 300 K temperatures where the  $dT_r$  becomes a significative contribution to  
 212 the  $\delta T$ , a further technological effort in the T-stability should be realised if the  $dF/F$



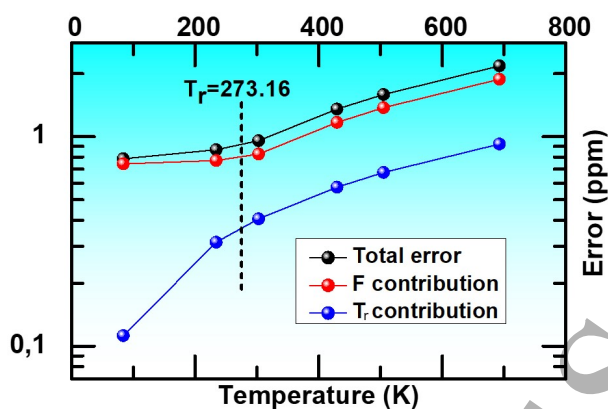


**Figure 3.** Total relative error on temperature measurement using LRT (black points), contribution due to  $T_r$  uncertainty (blue points) and contribution due to the  $F$  uncertainty (red points). The errors were calculated at ITS-90 fixed points using the ST transitions.

contribution will be improved better than 4 ppm. Finally for  $F$ , we evaluate that a few ppm  $F$ -measurement can be achieved by numerical integration of the absorption area for the spectra with S/N of thousands [25].

As a preliminary experimental support of this estimation on error in  $F$ , a spectroscopic measurement in the  $4.5 \mu\text{m}$  wavelength region was performed. Because we have not yet available a laser source resonant with the CO transitions in this spectral region, the test was realised on the  $(0^201-0^000)$  R(16)e transition of  $\text{N}_2\text{O}$  molecule at  $2209.0854 \text{ cm}^{-1}$ , which has similar spectroscopic characteristics to those the CO transitions at these wavelengths. Linear absorption spectroscopy of this transition was performed by interaction of a Quantum Cascade Laser (QCL) at  $4.5 \mu\text{m}$  with the  $\text{N}_2\text{O}$  gas contained in a cell of 18 cm of length at 1.1 mbar of pressure. Eleven consecutive transmission spectra were recorded by scanning the QCL frequency in an interval of about 500 MHz around  $\text{N}_2\text{O}$  resonance at acquisition times of 50 ms per spectrum. The results are reported in fig. 4 in terms of absorbance. Then, the integrated absorption (IA) area for each spectrum has been calculated by using numerical Romberg integration method and the area ratio  $\bar{R}$  with respect to the mean value were calculated, as well as the standard deviation. As a result a relative uncertainty on the absorbance area of about 1.1% was measured, only two times larger than we have prospected for spectra with a noise level  $\epsilon=0.05$  and a QCL linewidth of about 500 kHz [25]. We ascribe this discrepancy to temperature, pressure and absorption path fluctuations whose do not particularly taken care in this simple experimental set-up, differently of a real LRT set-up which provides simultaneous measurement of both transitions in a cell at a highly controlled temperature. In these conditions, error contributions due to absorption path and gas pressure fluctuations should be cancelled and highly minimised those due to temperature fluctuations. Hence, we are confident to achieve the prospected

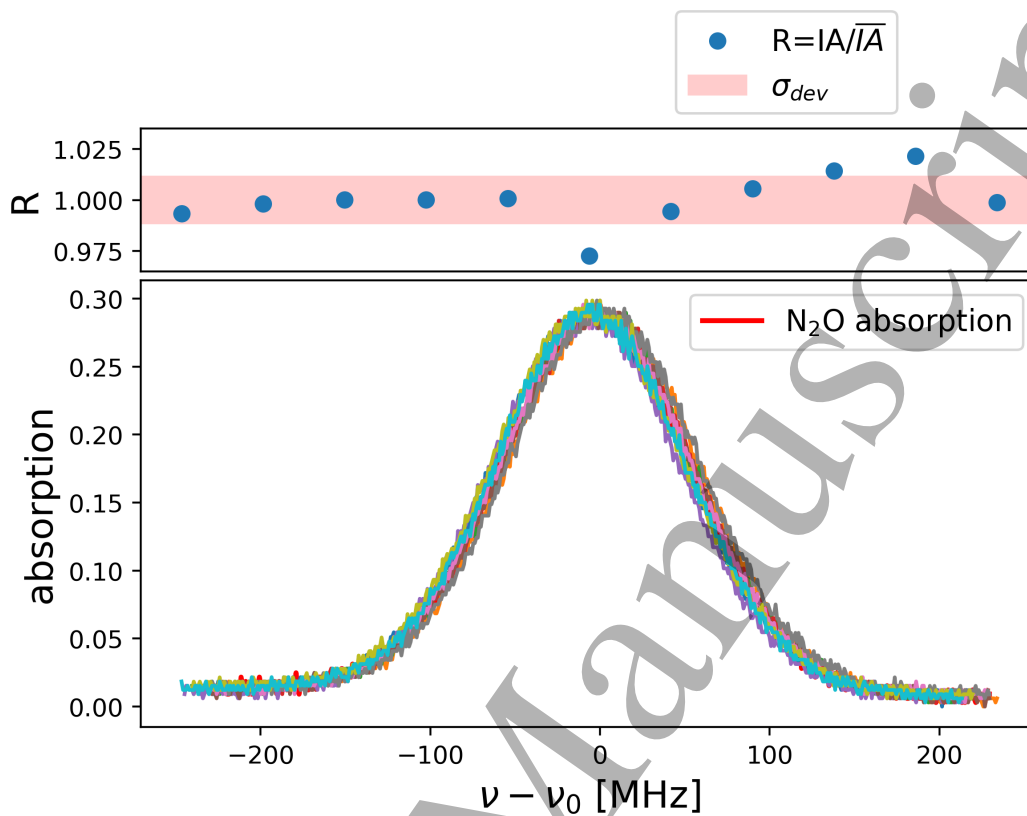


**Figure 4.** Absorption spectra of  $N_2O$  at  $2209.0854 \text{ cm}^{-1}$  in a 18 cm cell with a 1.1 mbar pressure when probed by a QCL at  $4.5 \mu\text{m}$ . The laser was frequency scanned around the resonance frequency and eleven different scans were recorded at 50 ms acquisition time. The integrated absorption (IA) area was calculated by using numerical Romberg integration method and the area ratio  $R$  (blue points) with respect to the mean value are plotted at the top of the figure, with the red bar indicated one standard deviation of such values.

$F$  uncertainties when the experiment will be performed in the conditions of the LRT method. Nevertheless,  $F$  measurement can be affected by systematic effects on the measured area due to the limited spectral range detected for each spectrum or due to the presence of off-resonance molecular absorbances different of the targeted ones. In the following, we evaluate the contributions of these systematics in view of a practical realisation of LRT in CO.

A benefit of LRT spectroscopy is the measurement of the absorbance of the different spectra without requiring a sophisticated line shape model, but just by numerical integration. In order to guarantee the few ppm  $F$ -accuracy in LRT methods, we evaluate that a scan bandwidth of about 2 GHz is sufficient to numerically capture the entire absorption area with a systematic error below ppm. The CO transition line-shapes in the thermodynamic conditions of the sample gas relevant for LRT experiments are due to Doppler broadening and pressure broadening.

The line shape  $I_D(\nu)$  due to Doppler broadening effect is given by:

$$I_D(\nu) = I_0 \sqrt{\frac{4 \ln(2)}{\pi}} \frac{1}{\Delta\nu_D} \text{Exp} \left( -4 \ln(2) \frac{(\nu - \nu_0)^2}{\Delta\nu_D^2} \right) \quad (3)$$

$$\Delta\nu_D = \frac{2\nu_0}{c} \sqrt{\frac{2kT \ln(2)}{m}} \quad (4)$$

where  $\nu_0$  is the line center frequency,  $m$  the CO mass,  $c$  vacuum light velocity and  $\Delta\nu_D$  FWHM Doppler linewidth contribution. Acquiring a 2 GHz absorption spectrum is sufficient to capture entire Doppler contribution, even in the case of the largest Doppler-broadening at the highest analyzed temperature ( $\Delta\nu_D=450$  MHz at 692.677 K). In fact, the difference between  $\int_{\nu_0-1\text{GHz}}^{\nu_0+1\text{GHz}} I_D(\nu)d\nu$  and  $\int_{-\infty}^{\infty} I_D(\nu)d\nu$  is 0.2 ppm in this case, and it decreases for the other temperatures in the analyzed range.

The pressure broadening generates a Lorentzian contribution to the line-shape:

$$I_L(\nu) \propto \frac{\gamma P}{(\nu - \nu_0)^2 + (\gamma P)^2} \quad (5)$$

where  $\gamma$  is pressure broadening coefficient [35]. For our analysis, we consider this profile at pressure  $P$  of about 10 Pascal, sufficient to have an adequate S/N of the absorption spectra of the  $ST$  and  $b$  transitions. If we consider each spectral profile separately to calculate  $S_a$  and  $S_b$  at  $T$  and  $T_r$ , a 2 GHz scan bandwidth is not sufficient to measure their area with the required precision because of the truncated-wings contribution. The error in this case is:

$$\frac{|\int_{-\infty}^{\infty} I_L(\nu)d\nu - \int_{\nu_0-1\text{GHz}}^{\nu_0+1\text{GHz}} I_L(\nu)d\nu|}{\int_{-\infty}^{\infty} I_L(\nu)d\nu} \simeq 336\text{ppm} \quad (6)$$

Even more, the error on  $R$  and  $R_r$  by considering  $R(T) = S_b(T)/S_a(T)$ , recorded with a 2 GHz scan, is:

$$\begin{aligned} & \frac{|\int_{\nu_0-1\text{GHz}}^{\nu_0+1\text{GHz}} R_r(\nu)d\nu - \int_{-\infty}^{\infty} R_r(\nu)d\nu|}{\int_{-\infty}^{\infty} R_r(\nu)d\nu} \simeq \\ & \simeq \frac{|\int_{\nu_0-1\text{GHz}}^{\nu_0+1\text{GHz}} R(\nu)d\nu - \int_{-\infty}^{\infty} R(\nu)d\nu|}{\int_{-\infty}^{\infty} R(\nu)d\nu} \simeq 60\text{ppm} \end{aligned} \quad (7)$$

and hence very far from the requested ppm. But the method is based on the ratio between to linestrength ratios,  $F$ . If the CO pressure  $P$  for the measurement of  $R$  was be exactly equal to the  $P$  for  $R_r$ , the error on  $F$  should be 0 even with a limited 2 GHz scan. If the  $P$  for measurement of  $R$  was be different to the  $P$  for  $R_r$ , the error on  $F$  should be 0 by using an infinite integration bandwidth. Assuming an error of 1% on the pressure gauge, the pressure broadening for  $R$  will be different of the pressure broadening of  $R_r$  and the error on  $F$  in the case of 2 GHz scan bandwidth is:

$$\frac{|\int_{\nu_0-1\text{GHz}}^{\nu_0+1\text{GHz}} F(\nu)d\nu - \int_{-\infty}^{\infty} F(\nu)d\nu|}{\int_{-\infty}^{\infty} F(\nu)d\nu} \simeq 0.59\text{ppm} \quad (8)$$

that is nearly one order of magnitude lower than error we considered on  $F$  of 4ppm across the present analysis. We can conclude that a 2 GHz scan bandwidth and an error of one per cent on the pressure gauge can be sufficient to candidate LRT as a ppm level primary thermometry technique.

The possible influence of interferent off-resonance absorptions to the measured area in the scan bandwidth is now evaluated. Thanks to the simple ro-vibrational spectrum of the biatomic molecule of CO, the chosen  $b$  transition at  $4263.837197 \text{ cm}^{-1}$  and the  $ST$  transitions (see Table 1) are very far apart of possible interfering absorptions. In the worst case, the nearest unwanted transition is the R(17) component of (3-1) band at  $4263.635524 \text{ cm}^{-1}$  ( $x$ -line) about 6.6 GHz apart from  $\nu_b$  and with a linestrength of  $6.261 \cdot 10^{-23} \text{ cm}^2/\text{mol}$ [35]. To estimate the contribution of the  $x$  transition wings to the integrated absorption of the  $b$  transition in a range of 2 GHz around  $\nu_b$ , we calculate the ratio between the expected contribution for the  $x$  and  $b$  absorptions when considering not interference from  $x$ :

$$x_{wing} = \frac{\int_{\nu_{0b}-1GHz}^{\nu_{0b}+1GHz} I_x(\nu) d\nu}{\int_{\nu_{0b}-1GHz}^{\nu_{0b}+1GHz} I_b(\nu) d\nu} \simeq 0.8ppm \quad (9)$$

which is again a contribution one order of magnitude lower than the prospected 4 ppm on  $F$ .

Finally, let us consider the uncertainty consequences on the  $F$  measurement when numerical integration of the spectra instead of lineshape fit is used to measure it. This consideration is not only important in terms that LRT is a line-shape model independent, avoiding, in this way, to accurately consider all velocity-changing collision effects, normally present in spectroscopy of gas species. Even in terms of how the uncertainty of the numerical integrated area is lower than fitted one. To evaluate it, we have simulated a Voigt profile of an absorption transition with a Doppler width contribution,  $\omega$  much larger than the collisional one and with an area  $A$ . This is the usual situation in optical spectroscopy-based thermometric techniques: LRT and Doppler Broadening Thermometry, DBT [38][38, 39]. A random white noise of the 1% was added to the spectral profile to simulate a real experimental spectrum of the transition. Then, we have determined the relevant spectral parameters for thermometry by using a fit procedure to measure  $\omega_F$  and  $A_F$ , and a numerical integration to measure  $A_I$ . The fit and numerical integration is repeated a significant number of times to get a normal statistical distribution of the measured parameters. As a result, the standard deviations of the fitted area ( $\sigma_{A_F}$ ) and Doppler linewidth contribution ( $\sigma_{\omega_F}$ ) are one order of magnitude worst than the numerical integrated area ( $\sigma_{A_I}$ ). Consequently, even if with an adequate line-shape model, better accurate results could be expected for LRT if compared with DBT due  $F$  is measured by the numerical integration and  $\omega$  by the fit procedure.

### 316 LRT on Er:YLF crystal: primary thermometry in the 9-100 K range

317 The use of the carbon monoxide for LRT is limited in the range 80 - 700 K because of  
 318 technical issues. Below 80 K, high resolution CO absorption spectroscopy is limited by  
 319 the gas sample vapour pressure at these T's. Above 700 K instead, the not negligible  
 320 absorption of interferences from off-resonance neighbour transitions limits the LRT-  
 321 application. A possible system useful to extend LRT range towards few Kelvin is a  
 322 rare-earth-doped crystal. In such materials, the shielding of f electrons by closed shells  
 323 makes possible optical transitions between these quasi-unperturbed f levels[40] with very  
 324 narrow achieved linewidths as, for example, the transitions of Erbium doped  $YLiF_4$   
 325 ( $Er^{3+} : YLF$ ) in the near-IR region[41, 42]. For this reason, we propose this crystal as  
 326 a target specie to perform LRT in the low temperature range of ITS-90.

327 In  $YLiF_4$ , erbium ions substitute yttrium ions in one crystallographic site of S4  
 328 point symmetry. Since  $Er^{3+}$  has an odd number of electrons, all crystal field levels are  
 329 doubly degenerate. In each  $^{2S+1}L_J$  multiplet, crystal field levels are characterized by  
 330 the absolute value of the projection of J number along crystal field axis, for example  
 331 the ground state energy level  $^4I_{15/2}$  is splitted by crystal field interaction in  $^4I_{15/2,|M_J|}$   
 332 where  $|M_J| = 5/2, 15/2, 3/2, 1/2, 9/2, 7/2, 11/2, 13/2$  each level is doubled degenerate  
 333  $|M_J| = |\pm M_J|$  and the degeneracy is removed if a magnetic field is applied.

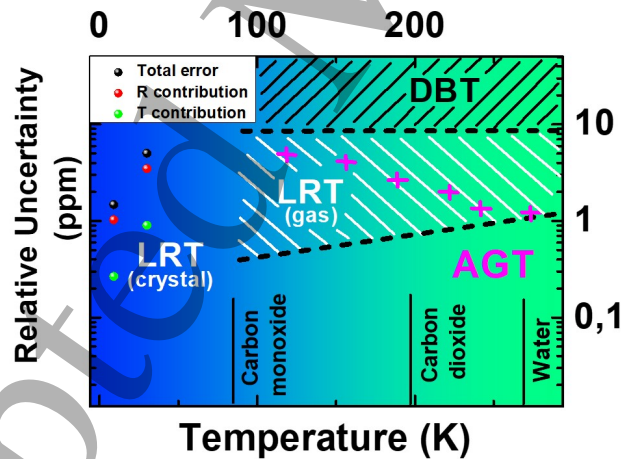


**Figure 5.** Relative T uncertainty (black points) and their partial contributions due to  $\delta T_r$  (green points) and  $\delta R$  for LRT applied to hyperfine transitions of Erbium doped  $YLiF_4$  crystal around 800 nm at T of 30 and 9 K with respect to the 100 K reference temperature. Uncertainty performances of AGT, DBT and LRT in the 80-300 K range are shown. Freezing points of CO, CO<sub>2</sub> and H<sub>2</sub>O are also indicated.

334 In order to evaluate the practical realization of LRT at the low temperatures of ITS-  
 335 90 scale, we estimated the errors contributing to the final temperature measurement by  
 336 considering the transitions  $^4I_{15/2,5/2} \rightarrow ^4I_{9/2,9/2}$  and  $^4I_{15/2,15/2} \rightarrow ^4I_{9/2,9/2}$  around 800 nm  
 337 as the *b* and *a* LRT-transitions, respectively. The starting level of the *b* transition is  
 338 the ground state and the starting level of *a* transition is  $17 \text{ cm}^{-1}$  above, equivalent to a  
 339 temperature of 24.5 K. Taking into account the  $S(T)$  values for the *a* and *b* transitions [43],

we calculate the ratios:  $R(T_r = 100K) = \frac{S_b(T_r)}{S_a(T_r)}$  and  $R(T) = \frac{S_b(T)}{S_a(T)}$  for  $T=30$  and  $9$  K. Consequently, as done above for the CO, the  $T$  and its total relative uncertainty from eqs. 1-2 and the partial uncertainties  $\delta T_r/T$  determination and  $\delta F/T$  were estimated (as for CO,  $\delta \nu_a/T$  is negligible if compared with the others). The results are shown in the left part of fig. 5. The same values and criteria as in CO are used for the  $dF$ ,  $dT_r$  and  $d\nu_a$  in this calculation. As a result, the total  $T$  uncertainty is few ppm proving the validity of LRT as primary thermometry technique also in few Kelvin range. This would be, to the best of our knowledge, the first optical primary thermometry technique working in this low temperature range. Indeed, in fig. 5 is also shown the range of applicability of the optical spectroscopy based PT's: DBT and LRT. DBT uses Doppler broadening due to the  $T$  of gas samples, and, in principle, a low temperature applicability up to  $80$  K could be prospected if CO is used $\parallel$ . LRT is also down limited to this  $T$  if CO is used, but its range of applicability can be extended up to  $9$  K if transitions in rare-earth doped materials as Erbium doped  $YLiF_4$  crystal are measured.

Comparison with the most accurate primary thermometry, Acoustic Gas Thermometry (AGT), in the range of  $80$ - $300$  K is also shown in fig. 5. Similar accuracies to the AGT ones are prospected for  $T$ 's around water triplet point and even better for low temperatures.

## Discussion

On the frame of the Kelvin unit dissemination prospected by *MeP-K-19* by using the ITS-90 scale corrected by the new PT's, we are advancing the LRT method as candidate for a no-contact primary thermometer. The thermometric capabilities of LRT envisage accuracies of thermodynamic temperature at the ppm level when applied to transitions of the CO molecule and of the Erbium doped  $YLiF_4$  crystal in a temperature range between  $80$  and  $700$  K and between  $9$  and  $100$  K, respectively. This accuracy makes LRT comparable even with the most precise PT's as those based in AGT. Even more, if compared with the other optical-based thermometry, the DBT [38], an accuracy improvement of a factor of  $15$  for  $T \simeq 300$  K is prospected. Discrepancies under mK level of  $T-T_{90}$  in  $9$ - $700$  K range can be tested by this accurate LRT thermometry, and in particular, the  $T$  range of meteorological interest [27]. In addition, LRT technique would be, to the best of our knowledge, the first optical based primary thermometry working at few kelvin with ppm accuracies. For the above discussion, crucial for LRT success as a primary thermometer is to achieve experimental accuracy at the few ppm level in the spectral measurements of  $F$  in a LRT experiment. The experimental feasibility of LRT is enabled by technological development of laser sources in near-infrared and mid-infrared with linewidths at the few kHz level (and less) reachable using different stabilization techniques as those based on ultra-stable cavities [44, 32] or whispering gallery mode

$\parallel$  A constant relative uncertainty of about  $9$  ppm was considered in all the range of applicability corresponding to that reported for  $CO_2$  at  $300$  K [38]. Different values could be achieved with different sample gases at other  $T$ 's.

microresonators [45, 46]. In addition, optical frequency comb (OFC) disciplined laser sources [47, 31] or directly OFC's as spectroscopic sources [48, 49, 50, 51] provide sub Hz control level of the absolute frequency.

## References

- [1] Bing Yang, Yang Yang Chen, Yong Guang Zheng, Hui Sun, Han Ning Dai, Xi Wen Guan, Zhen Sheng Yuan, and Jian Wei Pan. Quantum criticality and the Tomonaga-Luttinger liquid in one-dimensional Bose gases. *Physical Review Letters*, 2017.
- [2] Thomas M. Stace. Quantum limits of thermometry. *Physical Review A - Atomic, Molecular, and Optical Physics*, 2010.
- [3] Xibo Zhang, Chen-Lung Hung, Shih-Kuang Tung, and Cheng Chin. Observation of quantum criticality with ultracold atoms in optical lattices. *Science (New York, N.Y.)*, 2012.
- [4] Bretislav Friedrich, Bernhard Roth, Stephan Schiller, Susanne F Yelin, Dave Demille, Michael R Tarbutt, Jony J Hudson, Hendrick L Bethlem, Gerard Meijer, Francis Group, Guido Pupillo, Andrea Micheli, Thomas M Hanna, Hugo Martay, Dmitry S Petrov, Christophe Salomon, Georgy V Shlyapnikov, Francesca Ferlaino, Steven Knoop, Evgeny A Shapiro, Moshe Shapiro, Eliane Luc-koenig, Paul S Julienne, William C Stwalley, Phillip L Gould, Timur V Tscherbul, Roman V Krems, Goulven Quéméner, Naduvalath Balakrishnan, John L Bohn, and Jeremy M Hutson. COLD MOLECULES: Theory, Experiment, Applications. *Molecules*, 2009.
- [5] Alessandro Volpi and John L. Bohn. Magnetic-field effects in ultracold molecular collisions. *Physical Review A - Atomic, Molecular, and Optical Physics*, 2002.
- [6] L. Santamaria, V. Di Sarno, I. Ricciardi, M. De Rosa, S. Mosca, G Santambrogio, P Maddaloni, and P De Natale. Low-temperature spectroscopy of the  $12c2h2$  (1 + 3) band in a helium buffer gas. *The Astrophysical Journal*, 50:801, 2015.
- [7] A.J. Moerdijk, B.J. Verhaar, and A. Axelsson. Resonances in ultracold collisions of  $6Li$ ,  $7Li$ , and  $23Na$ . *Physical Review A*, 1995.
- [8] L. Santamaria, V. Di Sarno, P. De Natale, M. De Rosa, M. Inguscio, S. Mosca, I Ricciardi, Calonico D., F. Levi, and P Maddaloni. Comb-assisted cavity ring-down spectroscopy of a buffer-gas-cooled molecular beam. *Physical Chemistry Chemical Physics*, 18:16715–16720, 2016.
- [9] Marko T. Cvitaš, Pavel Soldán, Jeremy M. Hutson, Pascal Honvault, and Jean Michel Launay. Ultracold Li + Li<sub>2</sub> collisions: Bosonic and fermionic cases. *Physical Review Letters*, 2005.
- [10] Markus Greiner, Olaf Mandel, Tilman Esslinger, Theodor W. Hänsch, and Immanuel Bloch. Quantum phase transition from a superfluid to a mott insulator in a gas of ultracold atoms. *Nature*, 2002.
- [11] T. Donner, S. Ritter, T. Bourdel, A. Ottl, M. Kohl, and T. Esslinger. Critical Behavior of a Trapped Interacting Bose Gas. *Science*, 2007.
- [12] Immanuel Bloch, Jean Dalibard, and Wilhelm Zwerger. Many-body physics with ultracold gases. *Reviews of Modern Physics*, 2008.
- [13] M. de Podesta. The impact of the kelvin redefinition and recent primary thermometry on temperature measurements for meteorology and climatology. Report 125-O1, WMO technical conference on meteorological and environmental instruments and methods of observation, 2016.
- [14] R. Underwood, T. Gardiner, A. Finlayson, J. Few, J. Wilkinson, S. Bell, J. Merrison, J.J. Iverson, and M. de Podesta. A combined non-contact acoustic thermometer and infrared hygrometer for atmospheric measurements. *Met. Apps.*, 22:830–835, 2015.
- [15] Preston-Thomas H. The international temperature scale of 1990 (its-90). *Metrologia*, 27:3–10, 1990.
- [16] RL. Rusby, M. Durieux, AL. Reesink, RP. Hudson, G. Schuster, M. Kühne, WE. Fogle, RJ. Soulen, and ED. Adams. The provisional low temperature scale from 0.9 mk to 1k, plts-2000. *J. Low Temp. Phys.*, 126:633–642, 2002.

- [17] G. Machin. The kelvin redefined. *Meas. Sci. Technol.*, 29:022001, 2018.
- [18] J. Fischer. Low uncertainty boltzmann constant determinations and the kelvin redefinition. *Phil. Trans. R. Soc. A*, 374:20150038, 2016.
- [19] M. de Podesta, R. Underwood, G. Sutton, P. Morantz, P. Harris, D. F. Mark, F. M. Stuart, G. Vargha, and A. Machin. A low-uncertainty measurement of the boltzmann constant. *Metrologia*, 50:354–376, 2013.
- [20] C. Gaiser, B. Fellmuth, N. Haft, A. Kuhn, B. Thiele-Krivoi, T. Zandt, J. Fischer, O. Jusko, and W. Sabuga. Final determination of the boltzmann constant by dielectric-constant gas thermometry. *Metrologia*, 54(3):280, 2017.
- [21] N.E. Flowers-Jacobs, A. Pollarolo, K.J. Coakley, A.E. Fox, H. Rogalla, W. Tew, and S. Benz. A boltzmann constant determination based on johnson noise thermometry. *Metrologia*, 54(5):730–737, 2017.
- [22] L. Moretti, A. Castrillo, E. Fasci, M. De Vizia, G. Casa, G. Galzerano, A. Merlone, P. Laporta, and L. Gianfrani. Determination of the boltzmann constant by means of precision measurements of h218o line shapes at 1.39 $\mu$ m. *Physical Review Letters*, 111:060803, 2013.
- [23] G. Truong, J. D Anstie, E. F. May, T. M. Stace, and A. N. Luiten. Accurate lineshape spectroscopy and the boltzmann constant. *Nat. Commun.*, 6:8345, 2015.
- [24] B. Fellmuth, J. Fischer, G. Machin, S. Picard, P.P.M. Steur, O. Tamura, D. R. White, and H. Yoon. The kelvin redefinition and its mise en pratique. *Phil. Trans. R. Soc. A*, 374:20150038, 2016.
- [25] L. Santamaria Amato, M. Siciliani de Cumis, D. Dequal, G. Bianco, and P. Cancio Pastor. New precision spectroscopy based method for boltzmann constant determination and primary thermometry. *J. Phys. Chem. A*, 122(28):6026–6030, 2018.
- [26] J. Fischer, M. de Podesta, K. D. Hill, M. Moldover, L. Pitre, R. Rusby, P. Steur, O. Tamura, R. White, and L. Wolbe. Present estimates of the differences between thermodynamic temperatures and the its-90. *Int. J. Thermophys.*, 32:12, 2011.
- [27] R. Underwood, M. de Podesta, G. Sutton, L. Stanger, R. Rusby, P. Harris, P. Morantz, and G. Machin. Estimates of the difference between thermodynamic temperature and the international temperature scale of 1990 in the range 118 k to 303 k. *Phil. Trans. R. Soc. A*, 374:20150048, 2016.
- [28] Apurba Kumar Das, Mruthunjaya Uddi, and Chih-Jen Sung. Two-line thermometry and h2o measurement for reactive mixtures in rapid compression machine near 7.6 $\mu$ m. *Combustion and Flame*, 159(12):3493 – 3501, 2012.
- [29] Dy Svet. Comparison of classical methods of pyrometry for real bodies with a continuous emission spectrum. *High Temperature*, 3(3):407–&, 1965.
- [30] L. S. Rothman, C. P. Rinsland, and A.. Goldman. The hitran molecular spectroscopic database and hawks (hitran atmospheric workstation): 1996 edition. *Journal of Quantitative Spectroscopy and Radiative Transfer*, 60:665, 1998.
- [31] I. Galli, M. Siciliani de Cumis, F. Cappelli, S. Bartalini, D. Mazzotti, S. Borri, A. Montori, N. Akikusa, M. Yamanishi, G. Giusfredi, and *et al.* Comb-assisted subkilohertz linewidth quantum cascade laser for high-precision mid-infrared spectroscopy. *Appl. Phys. Lett.*, 102:121117, 2013.
- [32] I. Ricciardi, S. Mosca, M. Parisi, L. Santamaria, P. De Natale, and M. De Rosa. Sub-kilohertz linewidth narrowing of a mid-infrared optical parametric oscillator idler frequency by direct cavity stabilization. *Opt. Lett.*, 40:4743, 2015.
- [33] M. Siciliani de Cumis, S. Borri, G. Insero, I. Galli, A. Savchenkov, D. Eliyahu, V. Ilchenko, N. Akikusa, A. Matsko, L. Maleki, and *et al.* Microcavity-stabilized quantum cascade laser. *Laser Photonics Rev.*, 10:153–157, 2016.
- [34] P. Cancio, S. Bartalini, S. Borri, I. Galli, G. Gagliardi, G. Giusfredi, P. Maddaloni, P. Malara, D. Mazzotti, and P. De Natale. Frequency-comb-referenced mid-ir sources for next-generation environmental sensor. *Appl. Phys. B: Lasers Opt.*, 102:255–269, 2011.
- [35] I.E. Gordon *et al.* The hitran 2016 molecular spectroscopic database. *J. Quant. Spectrosc.*



*Radiat. Transfer*, 203:3–69, 201.

- [36] J.P. Bouanich, D Bermejo, J.L. Domenech, R. Z. Martinez, and J Santos. Pressure-induced lineshifts in the  $2 \leftarrow 0$  band of co self-perturbed and perturbed by he, kr,  $o_2$ , and  $n_2$ . *J. Mol. Spectrosc.*, 179:22–31, 1996.
- [37] S. L. Gilbert and Swann W. C. Carbon monoxide absorption references. *NIST Special Publication*, 50:801, 2002.
- [38] R. Gotti, L. Moretti, D. Gatti, A. Castrillo, G. Galzerano, P. Laporta, L. Gianfrani, and M. Marangoni. Cavity-ring-down doppler-broadening primary thermometry. *Phys. Rev. A: At., Mol., Opt. Phys.*, 97:012512, 2018.
- [39] Antonio Castrillo, Eugenio Fasci, Hemanth Dinesan, Stefania Gravina, Luigi Moretti, and Livio Gianfrani. Optical determination of thermodynamic temperatures from a  $c_2h_2$  line-doublet in the near infrared. *Phys. Rev. Applied*, 11:064060, Jun 2019.
- [40] A. Perrot, Ph. Goldner, D. Giaume, M. Lovri?, C. Andriamiadamanana, R.R. Goncalves, and Ferrier A. Narrow optical homogeneous linewidths in rare earth doped nanocrystals. *Phys. Rev. Lett.*, (111):203601, 2013.
- [41] R. Marino, I. Lorger, O. Guillot-Nol, H. Vezin, A. Toncelli, M. Tonelli, J.L. LeGout, and Ph. Goldner. Energy level structure and optical dephasing under magnetic field in  $er_3:liy_4$  at 1.5  $\mu m$ . *J. Lum.*, (169):478–482, 2016.
- [42] C. Braggio, G. Carugno, F. Chirossi, A. Di Lieto, M. Guarise, P. Maddaloni, A. Ortolan, G. Ruos, L. Santamaria, J. Tasseva, and M. Tonelli. Axion dark matter detection by laser induced fluorescence in rare earth doped materials. *Sci. Rep.*, (7):15168, 2017.
- [43] M.A. Couto dos Santos, Antic-Fidanceva E., Gesland J.Y., Krupac J.C., Lematre-Blaisea M., and Porcher P. Absorption and fluorescence of  $er$  doped  $liy_4$  : measurements and simulations. *Journal of Alloys and Compound*, 21:435–441, 1998.
- [44] I. Ricciardi, S. Mosca, P. Maddaloni, L. Santamaria, M. De Rosa, and P. De Natale. Phase noise analysis of a 10watt  $yb$ -doped fibre amplifier seeded by a 1-hz-linewidth laser. *Optics Express*, 21:14618–14626, 2013.
- [45] J Lim, A Savchenkov, E Dale, W Liang, D Elyahu, V Ilchenko, A B Matsko, Lute Maleki, and C W Wong. Chasing the thermodynamical noise limit in whispering-gallery-mode resonators for ultrastable laser frequency stabilization. *Nat. Commun.*, 8:8, 2016.
- [46] Simone Borri, Mario Siciliani de Cumis, Giacomo Insero, Saverio Bartalini, Pablo Cancio Pastor, Davide Mazzotti, Iacopo Galli, Giovanni Giusfredi, Gabriele Santambrogio, Anatoliy Savchenkov, Danny Elyahu, Vladimir Ilchenko, Naota Akikusa, Andrey Matsko, Lute Maleki, and Paolo De Natale. Tunable microcavity-stabilized quantum cascade laser for mid-ir high-resolution spectroscopy and sensing. *Sensors*, 16(2):238, 2016.
- [47] I Galli, S Bartalini, R. Ballerini, M Barucci, P Cancio, M De Pas, G Giusfredi, D Mazzotti, N Akikusa, and Po De Natale. Spectroscopic detection of radiocarbon dioxide at parts-per-quadrillion sensitivity. *Optica*, 3(4):385–388, 2016.
- [48] F Adler, M. J. Thorpe, K. C. Cossel, , and J. Ye. Cavity-enhanced direct frequency comb spectroscopy: technology and applications. *Annu. Rev. Anal. Chem.*, 3:175–205, 2010.
- [49] M Siciliani de Cumis, R Eramo, N Coluccelli, M Cassinero, G Galzerano, P Laporta, P De Natale, and P Cancio Pastor. Tracing part-per-billion line shifts with direct-frequency-comb vernier spectroscopy. *Phys. Rev. A*, 91(1):012505, 2015.
- [50] M Siciliani de Cumis, R Eramo, N Coluccelli, G Galzerano, P Laporta, and P Cancio Pastor. Multiplexed direct-frequency-comb vernier spectroscopy of carbon dioxide  $2\nu_1 + \nu_3$  ro-vibrational combination band. *J. Chem. Phys.*, 148:114303, 2018.
- [51] M. Vainio and L. Halonen. Mid-infrared optical parametric oscillators and frequency combs for molecular spectroscopy. *Phys. Chem. Chem. Phys.*, 18:4266–4294, 2016.

1  
2  
3  
4  
5 524 **Acknowledgements**  
6

7 525 The authors acknowledge partially financial support by: Project MOST funded by  
8 526 Agenzia Spaziale Italiana, project WhiTech funded by Agenzia Spaziale Italiana and  
9 527 Progetti di Ricerca di Interesse Nazionale (PRIN), Project No. 20152MRAKH of the  
10 528 Italian Ministry of University and Research. We acknowledged I. Galli for experimental  
11 529 support and discussions regarding N<sub>2</sub>O experimental test.  
12  
13  
14

15 530 **Additional information**  
16

17 531 Competing interests: The authors declare no competing interests.  
18  
19  
20  
21  
22  
23  
24  
25  
26  
27  
28  
29  
30  
31  
32  
33  
34  
35  
36  
37  
38  
39  
40  
41  
42  
43  
44  
45  
46  
47  
48  
49  
50  
51  
52  
53  
54  
55  
56  
57  
58  
59  
60